

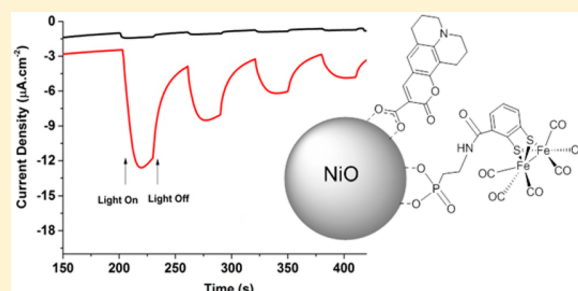
Dynamics and Photochemical H₂ Evolution of Dye–NiO Photocathodes with a Biomimetic FeFe-Catalyst

Liisa J. Antila,[†] Pedram Ghamgosar,^{†,‡} Somnath Maji,[§] Haining Tian, Sascha Ott, and Leif Hammarström*

Department of Chemistry—Ångström Laboratory, Uppsala University, Box 523, SE75120 Uppsala, Sweden

S Supporting Information

ABSTRACT: Mesoporous NiO films were cosensitized with a coumarin 343 dye and a proton reduction catalyst of the [Fe₂(CO)₆(bdt)] (bdt = benzene-1,2-dithiolate) family. Femto-second ultraviolet–visible transient absorption experiments directly demonstrated subpicosecond hole injection into NiO from excited dyes followed by rapid ($t_{50\%} \sim 6$ ps) reduction of the catalyst on the surface with a $\sim 70\%$ yield. The reduced catalyst was long-lived (2 μ s to 20 ms), which may allow protonation and a second reduction step of the catalyst to occur. A photoelectrochemical device based on this photocathode produced H₂ with a Faradaic efficiency of $\sim 50\%$. Fourier transform infrared spectroscopy and gas chromatography experiments demonstrated that the observed device deterioration with time was mainly due to catalyst degradation and desorption from the NiO surface. The insights gained from these mechanistic studies, regarding development of dye–catalyst cosensitized photocathodes, are discussed.



Molecular catalysts are attractive for solar fuels production because they can be both rapid and selective and require little material per active site. Their properties and interaction with the substrate can be tuned to a great extent via changes in their first and second coordination sphere, which offers great potential for rational design. To incorporate molecular catalysts into a device, one approach is to combine it with a dye-sensitized, mesoporous semiconductor film.^{1–6} Such dye-sensitized solar fuel devices (DSSFs) have attracted rapidly increasing interest, and several photoanodes based on TiO₂ or nano-ITO films and molecular water oxidation catalysts have been reported.^{1,3–5,7–9} For the corresponding photocathodes for H₂ production or CO₂ reduction, there are fewer examples, and the most common material is mesoporous NiO.^{10–23} In most cases the catalyst was not anchored to the NiO surface or was likely to detach upon reduction during the catalytic cycle. The photocathodes show poorer performance than the photoanodes, but so far very little detail on these systems has been given. From studies of solar cell materials, it is known that dye–NiO charge recombination is typically very rapid, often on a subnanosecond time scale,^{24–26} which is likely to hamper also the performance of DSSFs. Our group has previously shown that potential molecular catalysts, inspired by the active site of [FeFe]-hydrogenases, can be photoreduced by a dye on NiO.^{27,28} In the present work, we were able to make the first DSSF based on a biomimetic FeFe catalyst, on coumarin C343-sensitized NiO photoanodes, and demonstrate photochemical H₂

production. We give direct spectroscopic evidence that the catalyst is attached to the NiO surface and could monitor both its photoreduction and charge recombination.

DSSFs based on [2] showed poor NiO binding and negligible photocurrents in aqueous media (not shown). Therefore, [1] was prepared with a phosphonate group that was expected to allow for more stable binding to NiO and a longer linker that may slow charge recombination between the reduced catalyst and the NiO holes (Figure 1). The electronic properties should nevertheless be similar, with $E_{1/2} = -1.18$ V vs Fe^{+/0} for [2] in acetonitrile.²⁸ C343 absorbs mainly in the blue part of the spectrum but was chosen as dye for these

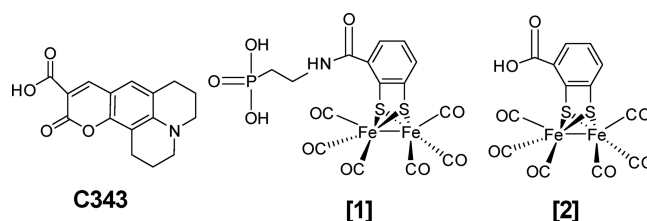


Figure 1. Structures of coumarin 343 (C343) and catalysts [1] and [2].

Received: October 6, 2016

Accepted: November 2, 2016

Published: November 2, 2016

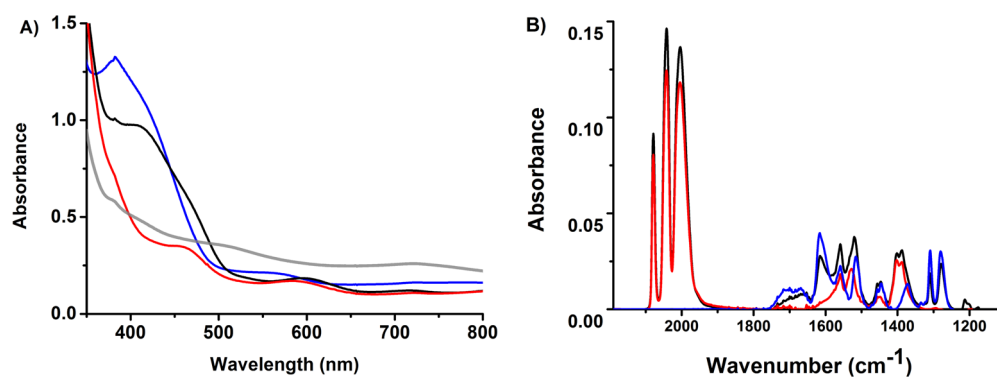


Figure 2. (A) UV-vis spectra and (B) FTIR spectra of the C343:[1] cosensitized NiO film (black line), [1]/NiO reference (red line), C343/NiO reference (blue line), and NiO film before sensitization (gray line, not shown in panel B).

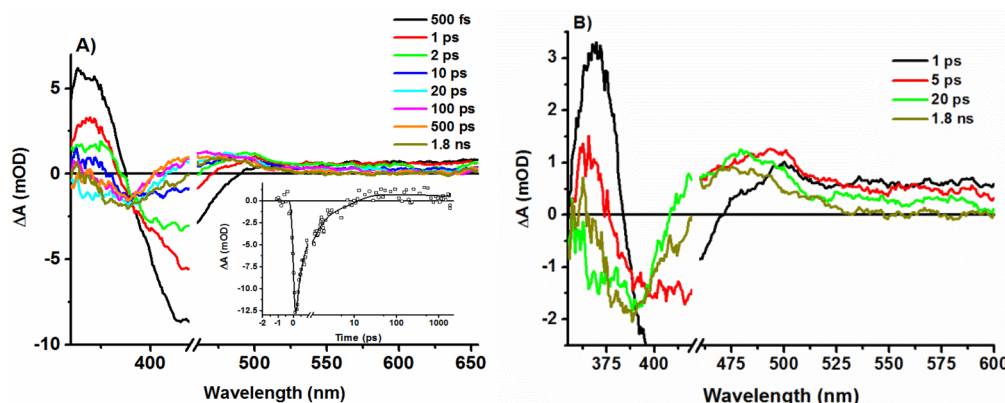


Figure 3. TA spectra of C343:[1]-cosensitized NiO after excitation at 440 nm (110 nJ, absorbed photon density 1.7×10^{15} photons/(cm² × pulse)) (A) 500 fs to 1.8 ns after excitation. (B) Magnified view of 1 ps to 1.8 ns after excitation. Inset in panel A shows time evolution of TA signal at 415 nm.

studies because it gives rapid hole injection into NiO; it has a suitable redox potential ($E^0(\text{C343}^{0/-}) \sim -1.6$ V vs $\text{Fc}^{+/0}$) in DMF²⁹ (see comment in ref 28); and its transient absorption spectra do not cover the band of the reduced catalyst (see below).

Figure 2A shows the ultraviolet–visible (UV–vis) absorption spectra of the NiO films sensitized with C343 dye and catalyst [1]. The C343-sensitized NiO (denoted C343/NiO) shows a dye absorption maximum around 400 nm, which is blue-shifted compared to the 422 nm absorption maximum reported earlier for C343 on NiO.³⁰ This is probably due to the different background absorption from the double-layered NiO film (Figure 2A), used in this study to increase loading of C343 and [1], compared to the single-layered film in ref 30. [1] on NiO ([1]/NiO) shows weak absorption bands centered at 450 and 600 nm, similar to those reported for the $[\text{Fe}_2(\text{bdt})(\text{CO})_6]$ complex in solution.³¹ The spectrum of the C343:[1]-cosensitized NiO film (C343:[1]/NiO) shows mixed features from the spectra of both C343/NiO and [1]/NiO references, namely, a broad band centered at ~ 450 nm and a weak band around 600 nm. Fourier transform infrared (FTIR) spectra measured for the samples are shown in Figure 2B. The vibrational peaks of the carbonyl groups³¹ of [1] at 2005, 2042, and 2079 cm⁻¹ in the spectra of the C343:[1]/NiO sample and the [1]/NiO reference verify the presence of [1] on the surface of the NiO film. By comparing the intensities of the vibrational peaks (at 2000–2100 cm⁻¹ for [1] and ca. 1300 cm⁻¹ for C343) in the cosensitized sample and in the two references

with a 1:1 C343:[1] solution (cf. ref 28), assuming that extinction coefficients for these bands are similar in solution and on NiO, we estimate that the relative concentrations of the dye and catalyst are between 1:2 and 2:1 in the C343:[1]/NiO sample.

Femtosecond transient absorption (TA) spectra obtained from the control samples, C343/NiO and [1]/NiO films, after exciting at 440 nm are presented in the Supporting Information. The 440 nm pump wavelength mainly excites the surface-bound C343 dye, although [1] also exhibits some absorption at this wavelength ($\epsilon(\text{C343}) = 15\,100 \text{ M}^{-1} \text{ cm}^{-1}$ vs $\epsilon([1]) = 1500 \text{ M}^{-1} \text{ cm}^{-1}$ at 440 nm).^{29,31} For the C343/NiO reference (Figures S2 and S3), the obtained results agree well with those reported by Morandeira et al.,³⁰ and a global fit with four exponentials gives time constants of <150 fs, 1 ps, 9 ps, and 1.2 ns. The amplitude spectrum of each lifetime component of the global fit constitutes a decay associated spectrum (DAS) that shows the transient absorption changes related to that component. On the basis of the DAS (Figure S3), the time constants are assigned to the hole injection from excited C343 dye to the valence band of NiO (<150 fs, formation of the $\text{C343}^{\bullet-}/\text{NiO}^{(+)}$ charge separated state) and to the recombination of the injected hole with the reduced $\text{C343}^{\bullet-}$ radical (9 ps). The DAS corresponding to the 1 ps time constant is assigned to the hole injection and recombination taking place in overlapping time scales, reflecting the heterogeneity of the sensitized nanoparticle film and the resulting complexity of the charge-transfer dynamics.³⁰ The

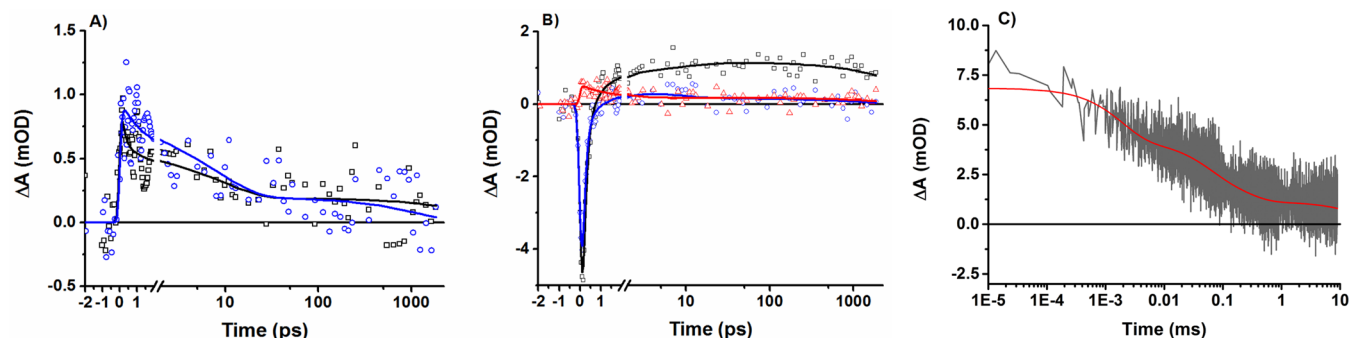


Figure 4. Time evolution of transient absorption after fs excitation (A) at 600 nm and (B) at 470 nm for C343:[1]/NiO (black squares and lines), C343/NiO (blue circles and lines), and [1]/NiO (red triangles and lines). (C) Time evolution of transient absorption after a 10 ns excitation pulse for C343:[1]/NiO at 470 nm. The red line is the fit with four exponentials to the experimental data: 1.9 μ s (38%), 52 μ s (24%), 230 μ s (20%), and >10 ms (17%).

spectrum at 1.2 ns shows a weak positive signal over the whole spectral range, with weak peaks around 350 and 475 nm, and represents a fraction of triplet excited C343.³⁰

The femtosecond TA spectra for the C343:[1]/NiO film in air are presented in Figure 3 (for more details, see Figures S4 and S5). The initial hole injection dynamics is rather similar to that of the C343/NiO reference, but the subsequent reaction is quite different. At 600 nm, where mainly the C343^{•+} radical absorbs (excited C343 has an isosbestic point here³⁰), the TA signal decays faster in the cosensitized sample than in the reference without the [1] catalyst (see Figure 4A). The decay is multiexponential with important contributions already at \sim 1 ps and continuing up to 1000 ps. In parallel, a new positive band between 410 and 500 nm and a negative band between 350 and 420 nm are observed to form \sim 1 ps after the excitation and persist beyond the time window of the measurement (Figure 3B). The positive band is very similar in shape and position to the flash–quench generated spectrum of singly reduced [Fe₂(bdt)(CO)₆]³¹ and is therefore assigned to the reduced [1] that persists beyond the time scale of this experiment ($\tau > 2$ ns).

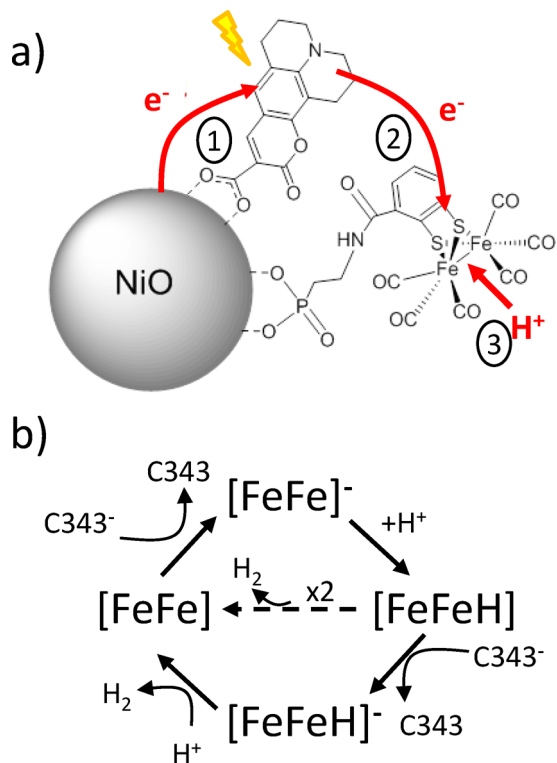
The DAS (Figures S5 and S6) and time evolution trace at 470 nm (Figure 4B) gives further insight into the formation dynamics of reduced [1]. In the C343/NiO reference, the TA signal at this wavelength corresponds to the quenching of the stimulated emission within 1 ps, which is followed by the decay of relatively weak positive absorption that is assigned to the reduced C343^{•+} radical (blue data). In the C343:[1]/NiO sample, the stimulated emission is quenched faster and the signal turns positive at 800 fs after excitation (black data). This positive TA signal does not decay significantly in the 2 ns time window of the measurement. A control experiment with the [1]/NiO reference shows only a weak positive signal at this wavelength (red data) that decays quite rapidly and is unrelated to the reduction of the catalyst (see Figure S7). Therefore, we can conclude that the reduction of the [1] catalyst requires the presence of the C343 dye on the surface of the NiO and cannot be carried out by direct excitation of [1] itself. As is clear from the TA spectra in Figure 3 and the traces in Figure 4, reduction of [1] by C343^{•+} is not single exponential. A half-time of $t_{50\%} \sim 6$ ps was estimated for this process from a plot of the 410–500 nm band maximum as a function of the delay time (see Figure S8). This is in agreement with the time evolution of the TA signal at 470 nm, which suggests that the catalyst reduction takes place mainly on the time scale of 1–10 ps. The yield of [1]^{•−} generation is therefore high: from the relative TA signals

of [1]^{•−} and C343^{•+}, we estimate a yield of \sim 70% for electron transfer from C343^{•+} to [1] (see the Supporting Information for details). This means that surface electron transfer from C343^{•+} to [1] competes favorably with recombination between C343^{•+} and NiO holes, which has ultrafast components ($\tau \sim 2$ ps;³⁰ see also above). The surface electron-transfer half-time is somewhat shorter and the yield somewhat higher than for the previously reported system C343:[2]/NiO for which $t_{50\%} \sim 10$ ps and a yield of 40–80% was reported.²⁸ However, by direct comparison of the TA signals in ref 28 with those in Figure 3, a yield of ca. 40% in that paper seems most consistent with the data. For both C343:[1]/NiO and C343:[2]/NiO, surface electron transfer is very rapid and there is no indication of dye–catalyst segregation or of isolated C343 molecules. It is interesting to note that the related process of hole hopping between dyes on mesoporous TiO₂ is typically several orders of magnitude slower.^{32–34} We propose that essentially each C343 dye on NiO is in close contact with a catalyst molecule in the cosensitized samples, so that surface electron transfer is a downhill, single-step process with a short electron-transfer distance. The flexible linking group of [1] may further facilitate close intramolecular contact. In contrast, many of the hole hopping studies on TiO₂ have involved multiple, self-exchange steps and may have been limited by steps on the heterogeneous surface where the transfer distance is longer.

To assess whether the reduced [1] catalyst is sufficiently long-lived for the first step of the water reduction process, namely, the protonation of the reduced catalyst, the lifetime of [1]^{•−} was recorded on a nano- to millisecond time scale. At 200 ns delay after laser flash excitation at 440 nm (10 ns, 2.6 mJ/cm²), the C343:[1]/NiO sample shows a strong transient absorption band between 400 and 510 nm (Figure S9), similar to what was observed at >10 ps in Figure 3. The decay of this signal at 470 nm clearly extends over several orders of magnitude (Figure 4c). Fitting of the TA signal required four exponentials, with roughly equal contributions, with time constants ranging from \sim 2 μ s to >10 ms (see Figure 4C caption). We suggest that the slower charge recombination compared to the case of [2] on NiO²⁸ is due to the longer linker group in [1]. According to Mirmohades et al.,³¹ protonation of the [Fe₂(bdt)(CO)₆][−] complex in acidic solutions may take place on the microsecond time scale; therefore, with a lifetime extending to the millisecond time scale, the reduced [1] should be able to undergo protonation with high yield. Scheme 1 illustrates the sequence of reactions

induced by single-photon absorption and suggests a mechanism for the catalytic cycle of [1].

Scheme 1. (a) Sequence of Photoinduced Electron-Transfer Reactions Observed and the Subsequent Protonation Suggested; (b) Suggested Mechanism of Proton Reduction by [1] under Photochemical Conditions, Supported by Data in Ref 31^a



^aDisproportionation of [FeFeH] (dashed line) is a conceivable alternative to the more intuitive, sequential ECEC mechanism (solid lines).

To evaluate the light response and proton reduction capacity of the sensitized NiO photocathodes, photoelectrochemical (PEC) experiments (Figure 5) were performed with a three-electrode system as described in the Supporting Information. The C343:[1]/NiO electrode in acetate buffer (pH 4.5) shows

a photocurrent response that is significantly higher than that of the C343/NiO reference, indicating that the photocurrent is due to proton reduction by the hydrogen evolution catalyst. Upon photoelectrolysis of the photocathode under -0.3 V vs Ag/AgCl and light illumination for 1100 s, produced hydrogen (H_2) could be detected in situ with a gas sensor and by gas chromatography–mass spectrometry (GC-MS). The corresponding data is shown in Figures 5B and S11. The photocathode based on C343:[1] produced 12.4 nmol of hydrogen, and the charge that passed through the circuit was 4.8 mC (Figure S10), which renders a Faradaic efficiency of ca. 50%. Thus, although the catalyst undergoes at most a few (≤ 3) turnovers during 1100 s, the initial photoelectrochemical H_2 evolution occurs with a decent Faradaic efficiency. The photocurrent density is, however, only ca. $10 \mu A cm^{-2}$, which is 3 orders of magnitude smaller than for an optimal system under full sun (ca. $10 mA cm^{-2}$). Poor light-harvesting of C343 (Figure 2A) can be expected to account for at least 1 order of magnitude losses. Another large loss factor is probably that charge recombination of the catalyst and NiO competes with protonation and second reduction of the catalyst. Each dye is excited at best only once per second under full sun, and for catalytic turnover to be more rapid than that, each catalyst must be reduced by several dyes in cooperation. Increasing the rate ratio of catalyst turnover and charge recombination is a major feature to consider in further design of dye-sensitized solar fuel devices. Obviously, a dye with a broader absorption spectrum in the visible would also be advantageous.

Notably, the photocurrent from the C343:[1]/NiO sample gradually decreased, which could be caused by catalyst decomposition. Rapid performance deterioration is still typical for dye-sensitized solar fuel devices.^{1–5} GC-MS experiments (Figure S11) confirm that CO ligands are released from C343:[1]/NiO during photoelectrolysis, which could be responsible for the gradual deactivation of the photocathode. Attenuated total reflection infrared (ATR-IR) spectra of C343:[1]/NiO before and after photoelectrolysis (Figure 6) further prove the degradation of catalyst by releasing CO ligands. The intensity of the three carbonyl bands of [1] around $1980–2100 cm^{-1}$ decreased to ca. one-third of their initial values during photoelectrolysis, while for example the carbonyl band of C343 ($\sim 1740 cm^{-1}$) was relatively unaffected. The decrease of the catalyst bands corresponds to the decrease of photocurrent by the end of the experiment (Figures 5A and S10). This

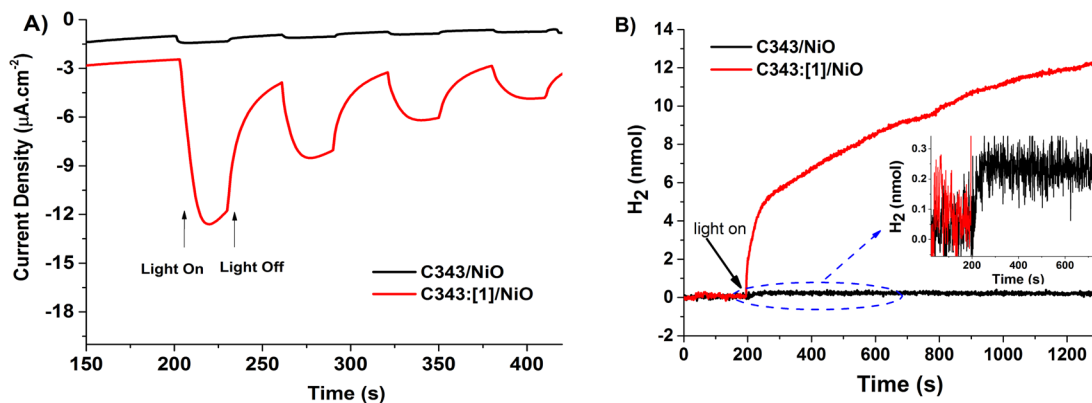


Figure 5. (A) Amperometric photocurrent density vs time recorded from the photocathodes at a bias of -0.3 V vs Ag/AgCl under chopped white light at an intensity of $100 mW/cm^2$ in pH 4.5 acetate buffer and (B) H_2 evolution under continuous photolysis. Black curves, C343/NiO; red curves, C343:[1]/NiO. Inset: magnified view of the data for C343/NiO.

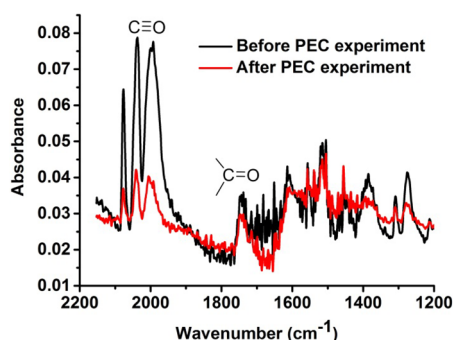


Figure 6. ATR-IR spectra of C343:[1]/NiO before (black) and after (red) the PEC experiments.

suggests that catalyst degradation is the main reason for the decrease in PEC activity of the photocathode.

To get more insight into the degradation of the catalyst during the PEC measurements, a similar C343:[1]/NiO sample on nonconducting CaF_2 was soaked in the pH 4.5 buffer first 1 h in the dark and then another hour under illumination. An FTIR spectrum of the sample was recorded before and after the soaking (Figure S12). From Figure S12 it is obvious that the buffer has little effect on the catalyst integrity as only small changes can be seen in the intensities of the IR peaks before and after soaking in the dark. In contrast, after soaking under illumination, the intensities of the three CO peaks at $\sim 2000\text{ cm}^{-1}$ decreased significantly. Also, the feature around 1400 cm^{-1} (associated only with [1], cf. Figure 2B) loses intensity upon soaking under illumination. This suggests that the catalyst is also desorbing from the NiO surface. In contrast, the C343 dye binding to the surface is not affected upon soaking and illumination as can be seen by the constant intensity of the C343 IR peaks at $\sim 1300\text{ cm}^{-1}$. These experiments strongly suggest that the catalyst [1] on C343-sensitized NiO is unstable under irradiation.

To conclude, we could directly demonstrate for the first time the critical electron-transfer processes between dye, catalyst, and NiO in a molecularly sensitized photocathode that is active for photoelectrochemical proton reduction to H_2 . Hole injection into NiO followed by ultrafast surface electron transfer led to rapid and efficient reduction of the catalyst [1]. Charge recombination of $[1]^-$ was slow, on the time scale of $2\text{ }\mu\text{s}$ – 20 ms , which may allow protonation and a second reduction step of the catalyst to occur. Thus, a device with C343:[1]/NiO as photocathode produced H_2 with a Faradaic efficiency of $\sim 50\%$. FTIR and GC experiments demonstrated that electrode degradation was mainly due to catalyst degradation. The mechanistic studies of sensitized photocathodes provide understanding for the processes and bottlenecks involved in this kind of system and should guide further work to improve their performance.

■ ASSOCIATED CONTENT

■ Supporting Information

The Supporting Information is available free of charge on the ACS Publications website at DOI: 10.1021/acsenergylett.6b00506.

Experimental details, synthesis of [1], additional experimental data, and analysis (PDF)

■ AUTHOR INFORMATION

Corresponding Author

*E-mail: leif.hammarstrom@kemi.uu.se.

Present Addresses

‡P.G.: Department of Engineering Sciences and Mathematics, Luleå University of Technology, Sweden.

§S.M.: Department of Chemistry, Indian Institute of Technology, Hyderabad, India

Author Contributions

†L.J.A. and P.G. contributed equally to the work.

Notes

The authors declare no competing financial interest.

■ ACKNOWLEDGMENTS

This work was supported by the Swedish Research Council, the Knut and Alice Wallenberg Foundation, and the Swedish Energy Agency.

■ REFERENCES

- (1) Youngblood, W. J.; Lee, S.-H. A.; Kobayashi, Y.; Hernandez-Pagan, E. A.; Hoertz, P. G.; Moore, T. A.; Moore, A. L.; Gust, D.; Mallouk, T. E. Photoassisted Overall Water Splitting in a Visible Light-Absorbing Dye-Sensitized Photoelectrochemical Cell. *J. Am. Chem. Soc.* **2009**, *131*, 926–927.
- (2) Tian, H. Molecular Catalyst Immobilized Photocathodes for Water/Proton and Carbon Dioxide Reduction. *ChemSusChem* **2015**, *8*, 3746–3759.
- (3) Hammarström, L. Accumulative Charge Separation for Solar Fuels Production: Coupling Light-Induced Single Electron Transfer to Multielectron Catalysis. *Acc. Chem. Res.* **2015**, *48*, 840–850.
- (4) Ashford, D. L.; Gish, M. K.; Vannucci, A. K.; Brennaman, M. K.; Templeton, J. L.; Papanikolas, J. M.; Meyer, T. J. Molecular Chromophore–Catalyst Assemblies for Solar Fuel Applications. *Chem. Rev.* **2015**, *115*, 13006–13049.
- (5) Yu, Z.; Li, F.; Sun, L. Recent Advances in Dye-Sensitized Photoelectrochemical Cells for Solar Hydrogen Production Based on Molecular Components. *Energy Environ. Sci.* **2015**, *8*, 760–775.
- (6) Willkomm, J.; Orchard, K. L.; Reynal, A.; Pastor, E.; Durrant, J. R.; Reisner, E. Dye-Sensitized Semiconductors Modified with Molecular Catalysts for Light-Driven H_2 Production. *Chem. Soc. Rev.* **2016**, *45*, 9–23.
- (7) Gao, Y.; Ding, X.; Liu, J.; Wang, L.; Lu, Z.; Li, L.; Sun, L. Visible Light Driven Water Splitting in a Molecular Device with Unprecedentedly High Photocurrent Density. *J. Am. Chem. Soc.* **2013**, *135*, 4219–4222.
- (8) Ashford, D. L.; Lapides, A. M.; Vannucci, A. K.; Hanson, K.; Torelli, D. A.; Harrison, D. P.; Templeton, J. L.; Meyer, T. J. Water Oxidation by an Electropolymerized Catalyst on Derivatized Mesoporous Metal Oxide Electrodes. *J. Am. Chem. Soc.* **2014**, *136*, 6578–6581.
- (9) Norris, M. R.; Concepcion, J. J.; Fang, Z.; Templeton, J. L.; Meyer, T. J. Low-Overpotential Water Oxidation by a Surface-Bound Ruthenium–Chromophore–Ruthenium–Catalyst Assembly. *Angew. Chem., Int. Ed.* **2013**, *52*, 13580–13583.
- (10) Li, L.; Duan, L.; Wen, F.; Li, C.; Wang, M.; Hagfeldt, A.; Sun, L. Visible Light Driven Hydrogen Production from a Photo-Active Cathode Based on a Molecular Catalyst and Organic Dye-Sensitized p-Type Nanostructured NiO. *Chem. Commun.* **2012**, *48*, 988–990.
- (11) Ji, Z.; He, M.; Huang, Z.; Ozkan, U.; Wu, Y. Photostable p-Type Dye-Sensitized Photoelectrochemical Cells for Water Reduction. *J. Am. Chem. Soc.* **2013**, *135*, 11696–11699.
- (12) Li, F.; Fan, K.; Xu, B.; Gabrielson, E.; Daniel, Q.; Li, L.; Sun, L. Organic Dye-Sensitized Tandem Photoelectrochemical Cell for Light Driven Total Water Splitting. *J. Am. Chem. Soc.* **2015**, *137*, 9153–9159.
- (13) Fan, K.; Li, F.; Wang, L.; Daniel, Q.; Gabrielson, E.; Sun, L. Pt-Free Tandem Molecular Photoelectrochemical Cells for Water

Splitting Driven by Visible Light. *Phys. Chem. Chem. Phys.* **2014**, *16*, 25234–25240.

(14) Click, K. A.; Beauchamp, D. R.; Huang, Z.; Chen, W.; Wu, Y. Membrane-Inspired Acidically Stable Dye-Sensitized Photocathode for Solar Fuel Production. *J. Am. Chem. Soc.* **2016**, *138*, 1174–1179.

(15) Kamire, R. J.; Majewski, M. B.; Hoffeditz, W. L.; Phelan, B. T.; Farha, O. K.; Hupp, J. T.; Wasielewski, M. R. Photodriven Hydrogen Evolution by Molecular Catalysts Using Al₂O₃-Protected Perylene-3,4-Dicarboximide on NiO Electrodes. *Chem. Sci.* **2016**, DOI: 10.1039/C6SC02477G.

(16) Kaeffer, N.; Massin, J.; Lebrun, C.; Renault, O.; Chavarot-Kerlidou, M.; Artero, V. Covalent Design for Dye-Sensitized H₂-Evolving Photocathodes Based on a Cobalt Diimine–Dioxime Catalyst. *J. Am. Chem. Soc.* **2016**, *138*, 12308–12311.

(17) Sahara, G.; Abe, R.; Higashi, M.; Morikawa, T.; Maeda, K.; Ueda, Y.; Ishitani, O. Photoelectrochemical CO₂ Reduction Using a Ru(II)–Re(I) Multinuclear Metal Complex on a p-Type Semiconducting NiO Electrode. *Chem. Commun.* **2015**, *51*, 10722–10725.

(18) Kou, Y.; et al. Visible Light-Induced Reduction of Carbon Dioxide Sensitized by a Porphyrin–Rhenium Dyad Metal Complex on p-Type Semiconducting NiO as the Reduction Terminal End of an Artificial Photosynthetic System. *J. Catal.* **2014**, *310*, 57–66.

(19) Sahara, G.; Kumagai, H.; Maeda, K.; Kaeffer, N.; Artero, V.; Higashi, M.; Abe, R.; Ishitani, O. Photoelectrochemical Reduction of CO₂ Coupled to Water Oxidation Using a Photocathode with a Ru(II)–Re(I) Complex Photocatalyst and a CoOx/TaON Photoanode. *J. Am. Chem. Soc.* **2016**, *138*, 14152–14158.

(20) Castillo, C. E.; et al. Visible Light-Driven Electron Transfer from a Dye-Sensitized p-Type NiO Photocathode to a Molecular Catalyst in Solution: Toward NiO-Based Photoelectrochemical Devices for Solar Hydrogen Production. *J. Phys. Chem. C* **2015**, *119*, 5806–5818.

(21) Gross, M. A.; Creissen, C. E.; Orchard, K. L.; Reisner, E. Photoelectrochemical Hydrogen Production in Water Using a Layer-by-Layer Assembly of a Ru Dye and Ni Catalyst on NiO. *Chem. Sci.* **2016**, *7*, 5537–5546.

(22) Bachmeier, A.; Hall, S.; Ragsdale, S. W.; Armstrong, F. A. Selective Visible-Light-Driven CO₂ Reduction on a p-Type Dye-Sensitized NiO Photocathode. *J. Am. Chem. Soc.* **2014**, *136*, 13518–13521.

(23) van den Bosch, B.; Rombouts, J. A.; Orru, R. V. A.; Reek, J. N. H.; Detz, R. J. Nickel-Based Dye-Sensitized Photocathode: Towards Proton Reduction Using a Molecular Nickel Catalyst and an Organic Dye. *ChemCatChem* **2016**, *8*, 1392–1398.

(24) Odobel, F.; Pellegrin, Y.; Gibson, E. A.; Hagfeldt, A.; Smeigh, A. L.; Hammarström, L. Recent Advances and Future Directions to Optimize the Performances of p-Type Dye-Sensitized Solar Cells. *Coord. Chem. Rev.* **2012**, *256*, 2414–2423.

(25) Gibson, E. A.; Smeigh, A. L.; Le Pleux, L.; Fortage, J.; Boschloo, G.; Blart, E.; Pellegrin, Y.; Odobel, F.; Hagfeldt, A.; Hammarström, L. A p-Type NiO-Based Dye-Sensitized Solar Cell with an Open-Circuit Voltage of 0.35 V. *Angew. Chem., Int. Ed.* **2009**, *48*, 4402–4405.

(26) Daeneke, T.; et al. Dominating Energy Losses in NiO p-Type Dye-Sensitized Solar Cells. *Adv. Energy Mater.* **2015**, *5*, 1401387.

(27) Gardner, J. M.; Beyler, M.; Karnahl, M.; Tschierlei, S.; Ott, S.; Hammarström, L. Light-Driven Electron Transfer between a Photosensitizer and a Proton-Reducing Catalyst Co-Adsorbed to NiO. *J. Am. Chem. Soc.* **2012**, *134*, 19322–19325.

(28) Brown, A. M.; Antila, L. J.; Mirmohades, M.; Pullen, S.; Ott, S.; Hammarström, L. Ultrafast Electron Transfer between Dye and Catalyst on a Mesoporous NiO Surface. *J. Am. Chem. Soc.* **2016**, *138*, 8060–8063.

(29) Hara, K.; Sato, T.; Katoh, R.; Furube, A.; Ohga, Y.; Shingo, A.; Suga, S.; Sayama, K.; Sugihara, H.; Arakawa, H. Molecular Design of Coumarin Dyes for Efficient Dye-Sensitized Solar Cells. *J. Phys. Chem. B* **2003**, *107*, 597–606.

(30) Morandeira, A.; Boschloo, G.; Hagfeldt, A.; Hammarström, L. Photoinduced Ultrafast Dynamics of Coumarin 343 Sensitized p-Type-Nanostructured NiO Films. *J. Phys. Chem. B* **2005**, *109*, 19403–19410.

(31) Mirmohades, M.; Pullen, S.; Stein, M.; Maji, S.; Ott, S.; Hammarström, L.; Lomoth, R. Direct Observation of Key Catalytic Intermediates in a Photoinduced Proton Reduction Cycle with a Diiron Carbonyl Complex. *J. Am. Chem. Soc.* **2014**, *136*, 17366–17369.

(32) Hu, K.; Robson, K. C. D.; Beauvilliers, E. E.; Schott, E.; Zarate, X.; Arratia-Perez, R.; Berlinguette, C. P.; Meyer, G. J. Intramolecular and Lateral Intermolecular Hole Transfer at the Sensitized TiO₂ Interface. *J. Am. Chem. Soc.* **2014**, *136*, 1034–1046.

(33) Brennan, B. J.; Durrell, A. C.; Koepf, M.; Crabtree, R. H.; Brudvig, G. W. Towards Multielectron Photocatalysis: A Porphyrin Array for Lateral Hole Transfer and Capture on a Metal Oxide Surface. *Phys. Chem. Chem. Phys.* **2015**, *17*, 12728–12734.

(34) Ardo, S.; Meyer, G. J. Direct Observation of Photodriven Intermolecular Hole Transfer across TiO₂ Nanocrystallites: Lateral Self-Exchange Reactions and Catalyst Oxidation. *J. Am. Chem. Soc.* **2010**, *132*, 9283–9285.